ce/papers
The online collection for conference papers in civil engineering
Ernst & Sohn A Wiley Brand

ORIGINAL ARTICLE

eurosteel SHEFFIELD 2021
Ernst & Sohn A Wiley Brand

Resistance of partially protected steel beams in fire

Janne Hautala, Iida Kangashaka, Mikko Malaska, Sami Pajunen

Correspondence

Associate Prof. Sami Pajunen
Tampere University
Unit of Civil Engineering
Kalevantie 4
33104 Tampere
Email: sami.pajunen@tuni.fi

Abstract

Intumescent coating is often used as a fire protection on steel members due to its attractive appearance and ease of use. In the case when the member is fully covered by the coating, the response during the fire can be predicted rather accurately. However, if the member is covered only partially, the member's temperature profile and the structural response during the fire are not trivial to define. Partially covered members appear e.g. in cases in which the member is coated on the building site, but some previously installed adjacent structures disturb the coating process. Such partially covered members have been studied in the literature mainly from the temperature point of view, but in the present paper, also the structural behavior during the fire is considered. The paper presents a general procedure how to define the resistance of a partially protected steel member during the fire. As a result, time-resistance curves are defined for bending, shear and torsion and standard IPE and HEA profiles are used in the example simulations and the results are compared to fully protected and unprotected cases. The finite element method is adopted both for the thermal and structural analyses. The expansion of the intumescent coating is taken into account using the so called effective thermal conductivity, hence the same model can be used for both analyses. The simulated temperature results are validated against experimental and simulation results from previous researches. The results for bending, shear and torsion resistance show, that when compared to the unprotected case, the partial protection increases the resistances and the improvement is at its height during 15-30 minutes from the beginning of the standard fire.

Keywords

Fire protection, Intumescent coating, Partial fire protection

1 Introduction

In some situations, when a steel beam is protected with intumescent coating, the profile cannot be covered on all sides. The Eurocode introduces some methods for calculating the bending and shear resistances of steel beams with non-uniform temperature gradients. Unfortunately, they are all for passive fire protection methods, and none of the protection cases apply to a beam with an unprotected flange [1].

Different ways to calculate the thermal conductivity of intumescent coating have been developed. Equivalent thermal conductivities have been studied in [2-7], where the foaming of the coating is modelled excplicitly. Effective thermal conductivity, where the expansion of the coating is calculated into the conductivity, has been modelled by [8], [9] and [3]. Finally, constant thermal conductivities have been researched by [10], [11] and [12].

The behaviour of steel columns in non-symmetrical fire has been studied by [13] and [14], and concrete filled steel tube columns in non-symmetrical fire were researched by [15-18]. Additionally, Schaumann et al. [19] have studied the temperature behaviour of a steel beam, which is protected by intumescent coating, but supports a trapezoidal steel sheet, which partially inhibits the coatings expansion. None of these examples include both the thermal and structural analysis of a partially protected steel profile. The studies done by Hautala et al. [20] and Kangashaka [21] presented in this paper aim to remedy this.

The profiles studied in this paper are IPE 200 and HEA 200. Three levels of fire protection are simulated for each profile; a fully protected, a partially protected, and an unprotected case. In the partially protected case the upper surface of the top flange is left unprotected. With each level of fire protection bending, shear, and torsion resistances are determined. From these results the effect of partial protection are compared to the protected and unprotected cases as a function of time. The simulations are done with ANSYS Workbench 19.2 [22].

2 The FEM-models

2.1 Material models and fire model

The effective thermal conductivity of the intumescent coating was calculated by dividing the equivalent thermal conductivity by Schaumann et al. [2] by a thermal expansion factor. The expansion factor (Figure 1) is the ratio between the thickness of the coating at time *i* and the original thickness [2]. The equivalent thermal conductivity is given in Equation (1) as

https://doi.org/10.1002/cepa.1495

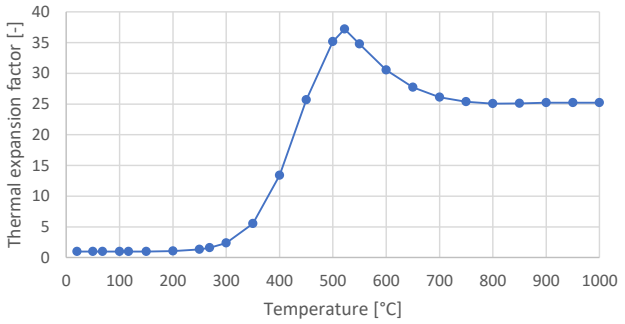

Figure 1: Thermal expansion factor of intumescent coating as a function of temperature [2, Fig. 3a]

$$\lambda_{eq} = \psi\left(\lambda_p + 4\sigma\theta_{IC}^3 d_p\right) + (1-\psi)\lambda_{IC}\,, \qquad (1)$$

In which λ_{eq} is the equivalent thermal conductivity [W/(mK)], ψ is the porosity [-], λ_p is the thermal conductivity of the trapped gas inside the pores [W/(mK)], σ is the Stefan-Boltzmann constant [W/(m^{2}K^4)], θ_{IC} is the temperature of IC [K], d_p is the diameter of the pores [m], and λ_{IC} is the thermal conductivity of IC at room temperature [W/(mK)]. The pore size is set to d_p = 1.2 mm [2], and they are assumed to contain nitrogen. According to Tabeling [23] λ_{IC} = 0.45 W/(mK). The porosity of the coating is calculated according to Equation (2) as

$$\psi(\theta) = \frac{\alpha-1}{\alpha}, \qquad (2)$$

where α is the thermal expansion factor [-]. The effective thermal conductivity λ_{eff} of the intumescent coating is calculated as

$$\lambda_{eff} = \frac{\lambda_{eq}}{\alpha}, \qquad (3)$$

where λ_{eq} is the equivalent thermal conductivity [W/(mK)] and α is the thermal expansion factor [-]. The density is ρ_{IC} = 1400 kg/m^3, and the specific heat of the coating was defined according to Figure 2 [2].

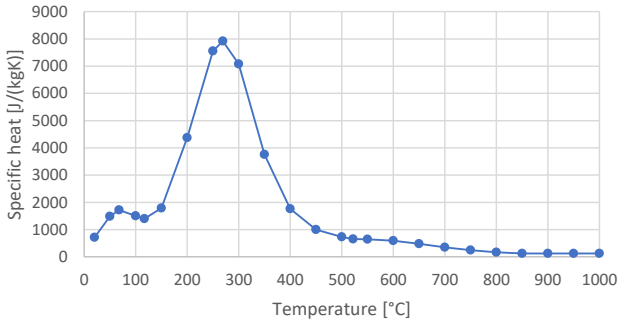

Figure 2: Specific heat of intumescent coating [2, Fig. 3b]

The specific heat, thermal conductivity, Young's modulus E_a, yield strength f_y of steel S 355 are from [1], as well as its temperature independent density ρ_a = 7850 kg/m^3. Steel is assumed to be linear elastic with linear strain hardening material. Tangent modulus is calculated as E_a/100 [24]. Poisson's ratio is υ_a = 0.3 [25].

The fire model used in the simulations is the ISO-834 standard fire curve, the coefficient of heat transfer by convection being α_c = 25 W/(m^{2}K) [27]. The emissivities are ε_{IC} = 0.8 for the intumescent coating [23], and ε_a = 0.7 for the unprotected steel surface [1].

2.2 Simulated models for bending, shear and torsion

A cantilever beam is used to model the bending, shear and torsion resistances. To determine the resistances, a fixed rotation or displacement was introduced at the free end of the beam, and the resistance was calculated from the beam's moment or force reaction at the supported end. In the bending model, the rotation φ_z (Figure 3a) around the z-axis was introduced, for the torsion model the rotation φ_x (Figure 3c) was around the x-axis, and in the shear model a displacement v (Figure 3b) in y-direction was used. In the torsion model, warping of the profile should be taken into account depending on the case, and in the current study, the warping is restrained in both ends of the model. For bending and torsion cases, the length L of the beam is 0.02 m. In case of shear resistance, the length must be so short that it eliminates the effect of the bending moment on the shear failure of the beam. This was checked using Equation 4 (when $M = FL$, and $Q = F$ at the support).

$$\frac{\sigma_{avg}}{\tau_{avg}} * 100\% = \frac{M*z}{2*I_y}\frac{A}{Q} * 100\% = \frac{FLzA}{2I_yF} * 100\% = \frac{LzA}{2I_y} * 100\%\,, \qquad (4)$$

where σ_{avg} is the average bending stress on the cross section [Pa], τ_{avg} is the average shear stress on the cross section [Pa], M is the maximum bending moment of the beam [Nm], z is the longest distance between the neutral axis and an edge of the cross section [m], A is the area of the beam cross section [m^2], I_y is the second moment of the cross-section [m^4] and Q is the maximum shear force of the beam [N]. Choosing L = 10 mm the ratio is below 10 % for both IPE 200 (7.3 %) and HEA 200 (6.9 %).

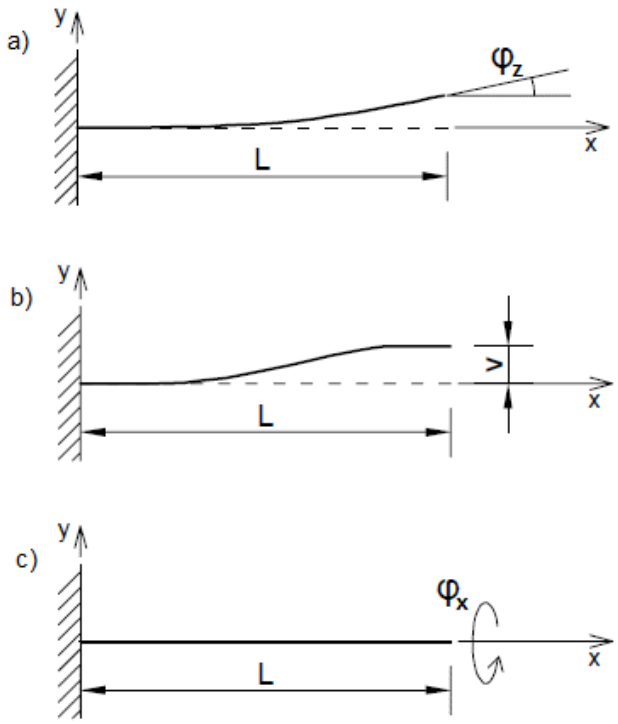

Figure 3: Mechanical models for a) bending, b) shear, and c) torsion

For each loading case (bending, shear, torsion) three models are made, a fully protected, a partially protected, and an unprotected model. The ISO-834 fire curve is applied on the beams, and a thermal analysis is performed. After this, the temperature gradients of each beam at heating times t = 0 s, 300 s, 450 s, 600 s, 900 s, 1200 s, 1500 s, 1800 s, 2100 s, 2400 s, 2700 s, 3000 s, 3300 s and 3600 s are used as body loads in structural analyses to determine the resistances at different heating times for each level of fire protection.

Each model comprises of two bodies, one for the steel profile and the other for the intumescent coating. Since the mechanical behavior is not of interest, the intumescent coating body is suppressed during the structural analyses. For each of the loading cases one end of the beam is supported so that the translation and rotation degrees-of-freedom are fixed. In the models for bending, translation is set to zero at the free end along the z-axis, and rotation is not allowed around the x- and y-axes. In the free end of the shear models, rotation is suppressed around all axes, and translation along the z-axis. In the torsion models, neither rotation nor translation was restricted at the free end. A rotation or a displacement is applied on the beams, which linearly changes from 0 to 0.6 degrees, or 0 to 0.06 mm during 0.6 s. The resulting moment or force reaction at the support are measured as a function of time. Additionally, for bending the plastic strain at the flanges, for shear the plastic strain at the web, and for torsion the plastic strain of the beam is measure as a function of time. Finally, the moment or force reaction is plotted as a function of the rotation or displacement. In the shear model for the partially protected HEA 200 at heating times 600 s, 900 s, 1200 s, 1500 s and 1800 s the beam was loaded for longer, since the plastic strain did not begin until after 0.6 s.

2.3 Elements and meshing

The elements used in this study are SOLID70 for thermal analysis and SOLID185 for structural analysis. The mesh size was determined from a sensitivity analysis (Figure 4). It was carried out by comparing the bending results of a fully protected IPE 200 beam at a heating time 1800 s. The mesh sizes were 1 mm, 2 mm, 3 mm, 4 mm, and 5 mm. The difference in results between 5 mm/4 mm meshing was significantly larger than between other meshes, which yielded relatively similar differences. Therefore, meshing size of 4 mm was chosen. Since none of the loads on the beams varied along the beams' lengths, there is only one element across the beam length. The meshes of the beams are depicted in Figures 5 and 6.

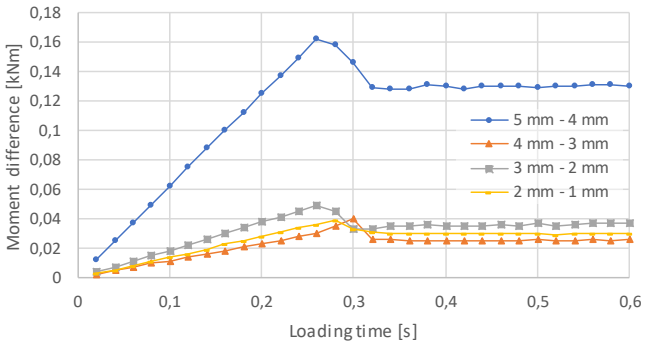

Figure 4: The differences in bending moment between consequent mesh sizes

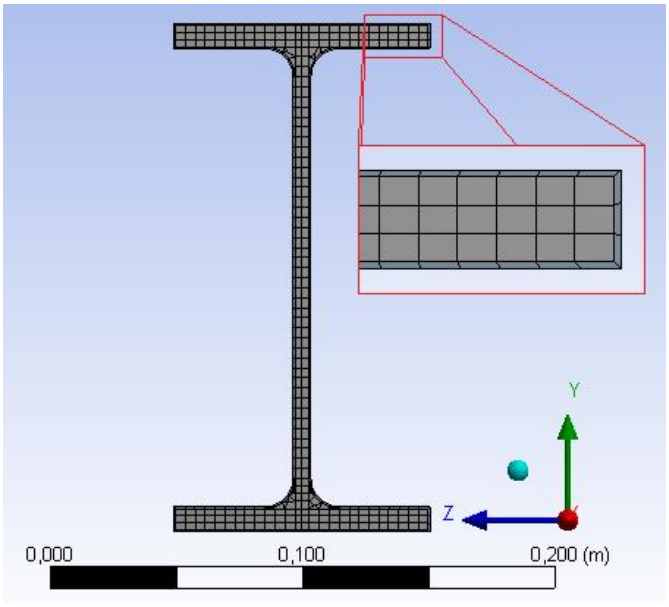

Figure 5: The finite element mesh for IPE 200

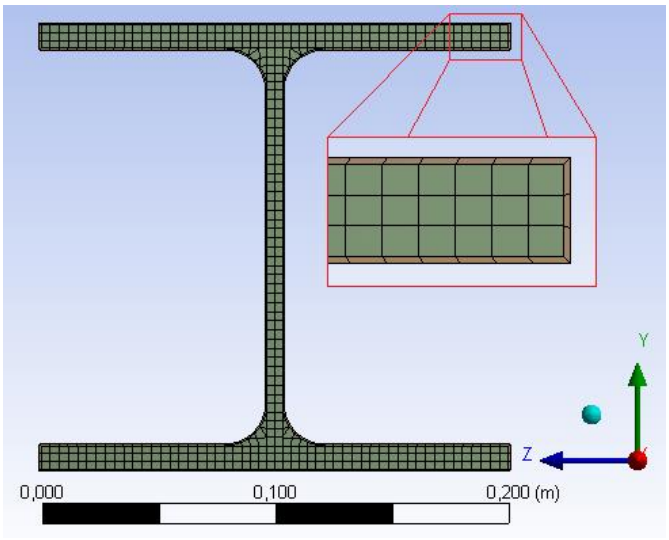

Figure 6: The finite element mesh for HEA 200

2.4 Validation of thermal simulation models

In their work, Schaumann et al. simulated the expansion of the intumescent coating and used the equivalent thermal conductivity [2]. The proposed simulation method was validated using their data, as well as test data from Tabeling [23]. They are shown in Figure 7. It also shows the ISO-834 fire curve and the temperature of the furnace in the Tabeling tests.

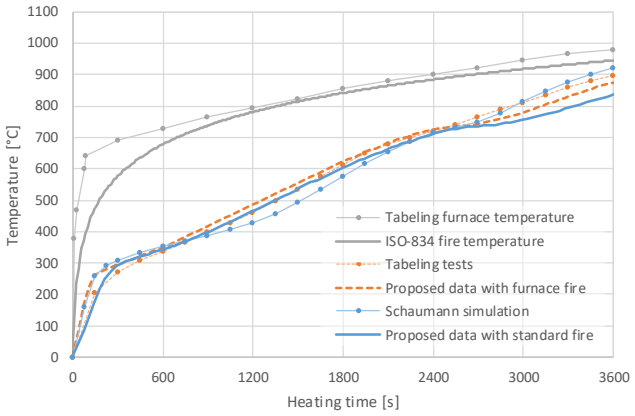

Figure 7: Validation of the model against data from previous research

As can be seen, the curves of the data from this study closely follow the data from previous studies. The maximum difference in temperature between the data from Schaumann et al. [2] and the proposed method with standard fire is 88.3 °C, and between the tests by Tabeling [23] and the proposed method with furnace fire it is 57.8 °C. The data can be assumed to validate the IPE 200 models, and since the profiles are so similar, the HEA 200 models are also validated.

3 Results

3.1 Temperatures

The results of the thermal analyses of the IPE 200 models are depicted in Figure 9. The temperature is shown as a function of time on the top flange (A), a quarter of the beam's height from the top (B), a quarter of the beam's height from the bottom (C), and the bottom flange (D) for all three levels of fire protection. These locations are shown in Figure 8.

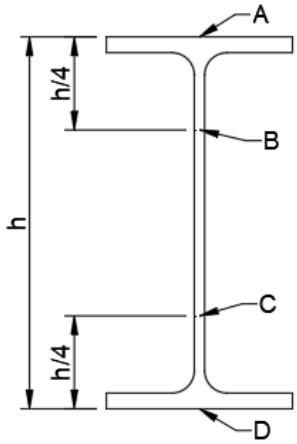

Figure 8: Locations of the points on the cross section

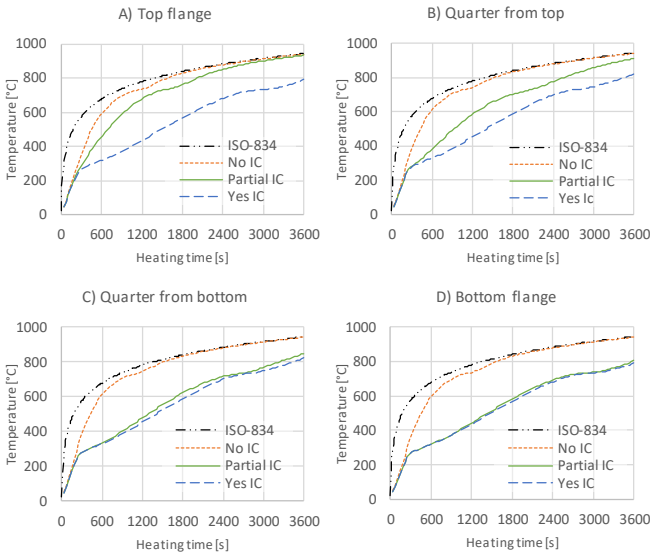

Figure 9: Temperatures of the IPE 200 beam at different locations on the cross section (A-D) and the ISO-834 fire curve

The curves for the unprotected beam and fully protected beam stay relatively still regardless of the location on the cross section. However, the curve for the partially protected beam shifts quite significantly depending on the location. As can be seen, at the bottom flange the temperatures of the partially and fully protected beams are practically the same. When moving from the bottom (D) towards the top flange (A), the temperature curve starts to better resemble the curve of the unprotected beam. Even though the IPE 200 beam heats up slightly faster, the temperature curves of IPE 200 and HEA 200 are so similar in shape, that the HEA 200 temperatures are not shown here.

3.2 Bending resistance

As mentioned earlier, the moment reactions of the supported end of the beam are plotted as a function of rotation. For the fully protected, partially protected, and unprotected IPE 200 beams they are shown in Figures 10, 11 and 12, respectively. From these curves the bending resistance at a certain heating time is read when the plastic strain reaches 0.2 %. These resistances are plotted as a function of heating time in Figure 13. The same is done for the HEA 200 beam, and the results are shown in Figure 14. To compare the results, the halving times (the time it takes for the resistance to reduce 50 %) of the resistances are shown in Table 1.

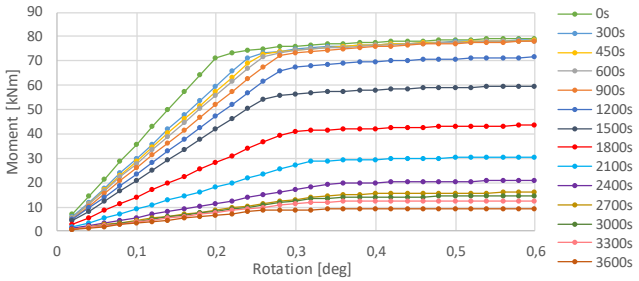

Figure 10: Bending moment in relation to rotation for a fully protected IPE 200 beam

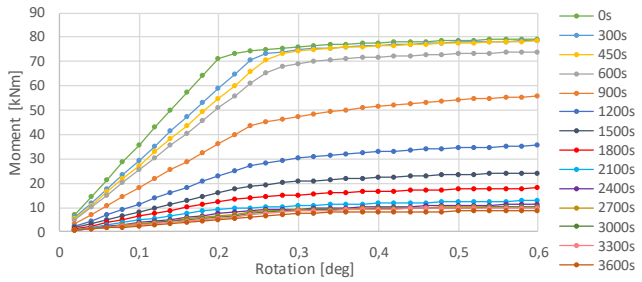

Figure 11: Bending moment in relation to rotation for a partially protected IPE 200 beam

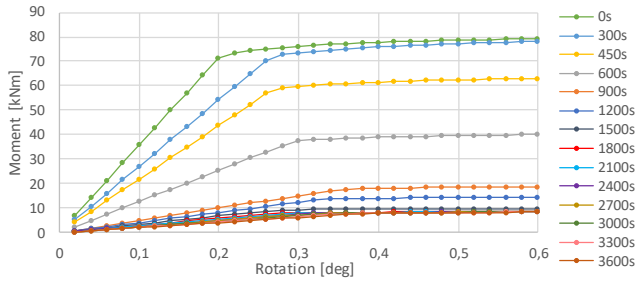

Figure 12: Bending moment in relation to rotation for an unprotected IPE 200 beam

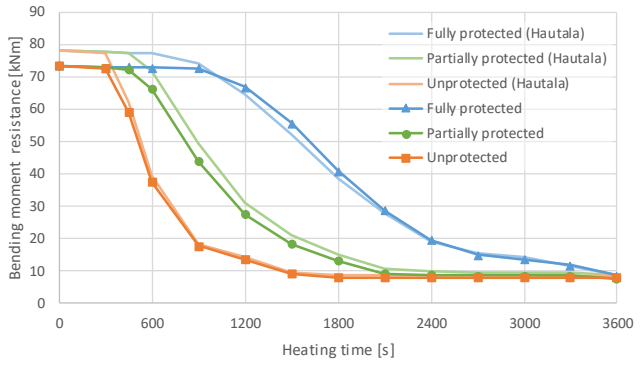

Figure 13: Bending moment resistance as a function of heating time for an IPE 200 beam. The results from previous research by Hautala et al. [20] are also included

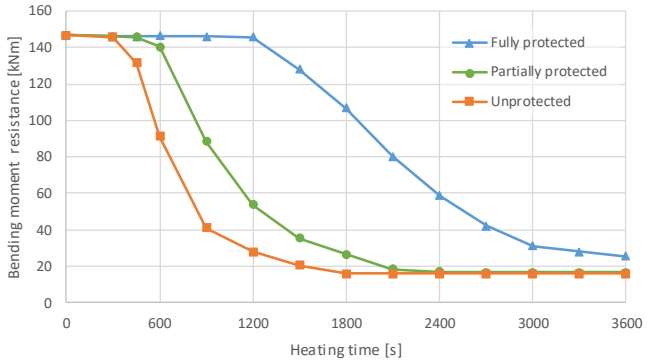

Figure 14: Bending moment resistance as a function of heating time for an HEA 200 beam

Table 1: Comparison of the halving times of bending resistances for IPE 200 and HEA 200

Fire protection	IPE 200 halving times	HEA 200 halving times	Differences in halving times
	Min	min	min
Fully protected	31.7	36.6	4.9
Partially protected	17.2	17.2	0.0
Unprotected	10.2	11.8	1.6

The difference in halving times between the fully protected beams follows from the fact that the IPE 200 beam heats up faster. However, the difference disappears when examining the partially protected beams. The partially protected beams heat up faster than the fully protected beams, and since the HEA 200 beam has larger flanges than the IPE 200 beam does, the increase in heating speed is also larger.

3.3 Shear resistance

Similarly to bending, the force reactions are plotted as a function of displacement for all three fire protection levels and for both beam types. From these curves, the shear force resistances are read when the plastic strain reaches 0.2 %, and they are plotted as a function of heating time (Figures 15 and 16). The halving times of the shear resistances are once again compared in Table 2.

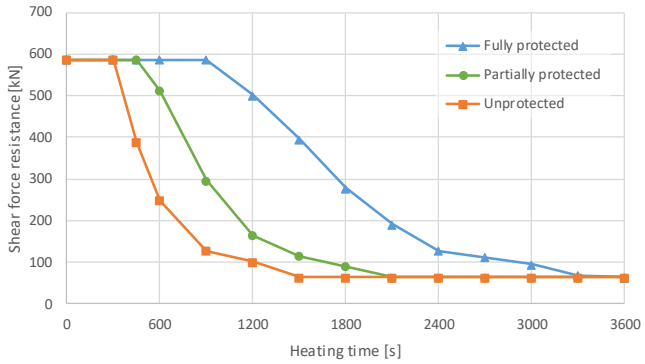

Figure 15: Shear force resistance as a function of heating time for an IPE 200 beam

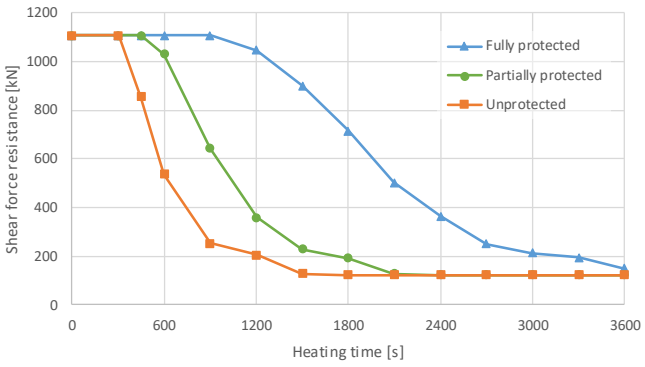

Figure 16: Shear force resistance as a function of heating time for an HEA 200 beam

Table 2: Comparison of the halving times of shear resistances for IPE 200 and HEA 200

Fire protection	IPE 200 halving times	HEA 200 halving times	Differences in halving times
	Min	min	min
Fully protected	29.3	33.8	4.5
Partially protected	15.1	16.5	1.4
Unprotected	9.2	9.9	0.7

As for bending, the difference between the halving times of the fully protected beams is quite large because IPE 200 is heating up faster. However, the halving times of the partially protected beams are no longer the same. This is likely due to the fact that shear is manly carried by the web of the cross section.

3.4 Torsion resistance

Finally, the torsion resistance curves as a function of heating time are plotted as before. They are presented in Figure 17 and 18. The halving times are compared in Table 3.

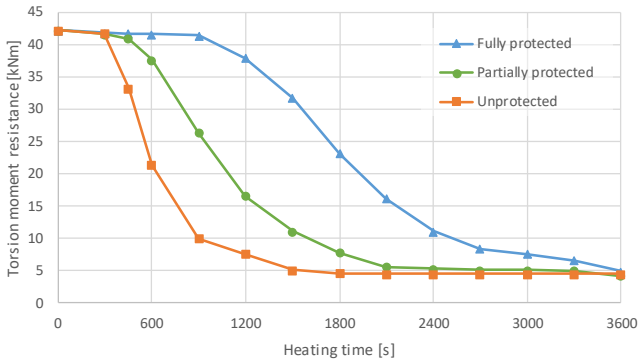

Figure 17: Torsion moment resistance as a function of heating time for an IPE 200 beam

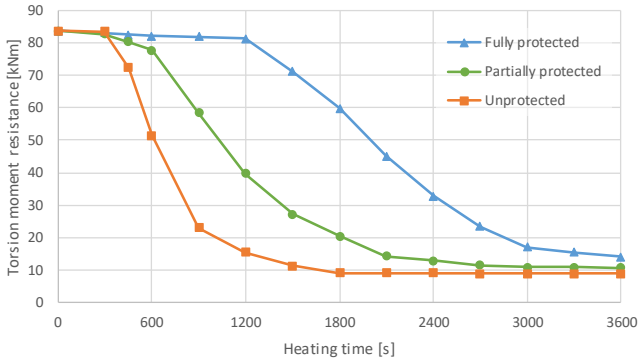

Figure 18: Torsion moment resistance as a function of heating time for an HEA 200 beam

Table 3: Comparison of the halving times of torsion resistances for IPE 200 and HEA 200

Fire protection	IPE 200 halving times	HEA 200 halving times	Differences in halving times
	min	min	min
Fully protected	31.5	36.3	4.8
Partially protected	17.7	19.4	1.7
Unprotected	10.1	11.7	1.6

Once again, the difference between the halving times of the fully protected beams is explained with the fact that the IPE 200 is heating up faster. After this, however, the differences for partially protected and unprotected beams are rather similar. After the increase in heating speed caused by removing the intumescent coating from the upper flange, it seems that the shape of the cross section affects the halving time more than the higher and more even temperature distribution caused by removing all intumescent coating. Since the torsion modulus of the HEA 200 beam is higher, its halving times are also higher.

4 Conclusions

In this study, the effect of partial fire protection on the bending, shear and torsion resistances of IPE 200 and HEA 200 beams in a standard fire was studied. Based on previous studies partially protected beams have lower resistances than fully protected beams, but their resistances do not decrease quite as quickly as those of unprotected beams. In this paper it was found that the halving times of the partially protected beams were several minutes longer than those of the unprotected beams. The proposed method provides information on the performance of partially protected structures more broadly, and can thus be used in design universally, and not just in designing cantilever beams. Therefore, the advantage provided by partial protection should be utilized when designing the fire performance of structures.

References

[1] SFS-EN 1993-1-2. Eurocode 3: Design of steel structures. Part 1-2: General rules. Structural fire design. Helsinki 2005, Suomen Standardoimisliitto SFS ry. 82 p.

[2] Schaumann, P., Tabeling, F., Weisheim, W. Fire design of steel structures with intumescent coatings. Nordic Steel Construction Conference, Tampere, Finland, September 23-25, 2015.

[3] Wang, Y., Göransson, U., Holmstedt, G., Omrane, A. A model for prediction of temperature in steel structure protected by intumescent coating, based on tests in the cone calorimeter. 8th International Symposium on Fire Safety Science, Bei-jing, China, September 18-23, 2005. pp. 235-246.

[4] Griffin, G.J. The modeling of heat transfer across intumescent polymer coatings. Journal of Fire Sciences 28(2010)3, pp. 249-277.

[5] Mao, C.H., Othuman Mydin, M.A., Que, X.B. Analytical model to establish the thermal conductivity of porous structure. Jurnal Teknologi 69(2014)1, pp. 103-111.

[6] Zhang, Y., Wang, Y.C., Bailey, C.G., Taylor, A.P. Global modelling of fire pro-tection performance of an intumes-

cent coating under different furnace fire condi-tions. Journal of Fire Sciences 31(2013)1, pp. 51-72.

[7] Zhang, Y., Wang, Y.C., Bailey, C.G., Taylor, A.P. Global modelling of fire pro-tection performance of intumescent coating under different cone calorimeter heating conditions. Fire Safety Journal 50(2012), pp. 51-62.

[8] Bartholmai, M., Schartel, B. Assessing the performance of intumescent coatings using bench-scaled cone calorimeter and finite difference simulations. Fire and Materials 31(2007)3, pp. 187-205.

[9] Staggs, J.E.J. Thermal conductivity estimates of intumescent chars by direct nu-merical simulation. Fire Safety Journal 45(2010), pp. 228-237.

[10] Li, G-Q., Han, J., Lou, G-B., Wang, Y.C. Predicting intumescent coating pro-tected steel temperature in fire using constant thermal conductivity. Thin-Walled Structures 98(2016), pp. 177-184.

[11] Li, G-Q., Lou, G-B., Zhang, C., Wang, L-L., Wang, Y-C. Assess the fire re-sistance of intumescent coatings by equivalent constant thermal resistance. Fire Technology 48(2012), pp. 529-546.

[12] Zhang, C. Reliability of steel columns protected by intumescent coatings sub-jected to natural fires. Doctoral Thesis. Berlin 2015. National Institute of Stand-ards and Technology, USA. 140 p.

[13] Agarwal, A., Choe, L., Varma, A.H. Fire design of steel columns: Effects of thermal gradients. Journal of Constructional Steel Research 93(2014), pp. 107-118.

[14] Wang, P., Xia, J., Du, Q. Temperature rise of a protected steel column exposed to fire from two adjacent sides. Fire Technology 52(2016)6, pp. 1887-1914.

[15] Guo, H., Long, X., Yao, Y. Fire resistance of concrete filled steel tube columns subjected to non-uniform heating. Journal of Constructional Steel Research 128(2017), pp. 542-554.

[16] Heinisuo, M., Jokinen, T. Tubular composite columns in a non-symmetrical fire. Magazine of Civil Engineering 49(2014)5, pp. 107-120.

[17] Yang, H., Liu, F., Zhang, S., Lv, X. Experimental investigation of concrete-filled square hollow section columns subjected to non-uniform exposure. Engineering Structures 48(2013), pp. 292-312.

[18] Yang, H., Liu, F., Gardner, L. Performance of concrete-filled RHS columns ex-posed to fire on 3 sides. Engineering Structures 56(2013), pp. 1986-2004.

[19] Schaumann, P., Tabeling, F., Weisheim, W. Numerical simulation of the heating behaviour of steel profiles with intumescent coating adjacent to trapezoidal steel sheets in fire. Journal of Structural Fire Engineering 7(2016)2, pp. 158-167.

[20] Hautala, J., Pajunen, S., Mela, K., Heinisuo, M. Resistance of partially intumes-cent covered steel member in fire. 17th International Conference on Computing in Civil and Building Engineering, Tampere, Finland, June 5-7, 2018.

[21] Kangashaka, I. The bending, shear and torsion resistances of partially protected beams in fire. Master's Thesis. Tampere 2019. Tampere University. 59 p.

[22] ANSYS Workbench, version 19.2, ANSYS, Inc.

[23] Tabeling, F. Zum Hochtemperaturverhalten dämmschichtbildender Brandschutz-systeme im Stahlbau (in English: High temperature behaviour of intumescent coating on steel constructions). Doctoral Thesis. Hannover 2014. Leibniz Uni-versitaet Hannover. 312 p.

[24] SFS-EN 1993-1-5. Eurocode 3. Design of steel structures. Part 1-5: Plated struc-tural elements. Helsinki 2006. Suomen Standardoimisliitto SFS ry. 55 p.

[25] SFS-EN 1993-1-1. Eurocode 3: Design of steel structures. Part 1-1: General rules and rules for buildings. Helsinki 2005, Suomen Standardoimisliitto SFS ry. 98 p.

[26] Salmi, T., Pajunen, S. Lujuusoppi. Tampere 2010, Pressus. 462 s.

[27] SFS-EN 1991-1-2. Eurocode 1: Actions on structures. Part 1-2: General actions. Actions on structures exposed to fire. Helsinki 2003, Suomen Standardoimisliitto SFS ry. 61 p.